1.D.2 *Nuclear Physics* **A249** (1975) 141–165, © *North-Holland Publishing Co , Amsterdam*

COLLECTIVE MODEL DESCRIPTION OF TRANSITIONAL ODD-A NUCLEI †

(II). Comparison with unique parity states of nuclei in the $A = 135$ and $A = 190$ mass regions

J MEYER-TER-VEHN††

Lawrence Berkeley Laboratory, University of California
Berkeley, California 94720

Received 17 February 1975
(Revised 22 April 1975)

Abstract: Recent experimental data on unique-parity spectra of odd-A nuclei in the $A = 135$ and $A = 190$ mass regions are compared in a systematic way with calculated energies and transition probabilities of a quasiparticle coupled to a rotating *triaxial* core The comparison yields detailed evidence for triaxial shapes Complex spectra of strongly coupled stucture as well as decoupled structure and various intermediate types are reproduced by the model with core parameters β and γ determined from neighbouring even nuclei The coexistence of $\Delta I = 2$ and $\Delta I = 1$ band structures, seen in some of the experimental spectra, is explained as a consequence of the shape asymmetry In the $A = 190$ region, the odd-A spectra confirm the existence of a gradual shape transition from prolate-type shapes (^{186}Os, $\gamma = 16°$) to oblate-type shapes (^{198}Hg, $\gamma = 37°$) Energies and lifetimes in $A \approx 135$ nuclei reveal prolate triaxial shapes with γ-values in the range $20° < \gamma < 30°$. Contrary to the expectation of very γ-soft, fluctuating shapes which is based on calculated collective potentials, the present work seems to indicate that a number of transitional nuclei may have rather stable triaxial shapes

1. Some general remarks

This is the second part of a collective model study on odd-A transitional nuclei In part I [ref [1])], the model of a single-j quasiparticle coupled to a rotating triaxial core has been investigated A general survey about the calculated energies, moments and transition probabilities has been given there including a physical interpretation of the results. In this second part, a systematic comparison of the model calculation with unique-parity states of transitional odd-A nuclei in the $A = 190$ and $A = 135$ mass regions is presented

It should be emphasized from the beginning that the assumption of rigid triaxial shapes with fixed shape parameters β and γ is considered as an approximation to the actual nuclear wave functions Against the general belief – and also unexpected for the author of the present work – this assumption turns out to be a very useful approximation which is well supported by new data most of them obtained from heavy-ion

† Work performed under the auspices of the US Atomic Energy Commission and supported in part by the Deutsche Forschungsgemeinschaft

†† On leave of absence from Physik-Department, Technische Universitat Munchen, Munchen, West Germany

experiments during the last three years They give new support to the old Davydov model and seem to indicate that a number of transitional nuclei have triaxial shapes which are more stable than expected from theoretical potential-energy surfaces. This point will be discussed in sect. 4

In particular, this paper wants to show (i) that the triaxial model seems to reproduce *all* experimental states (below 2Δ, Δ being the pairing gap) of certain families of unique-parity states in almost the right level order and (ii) that it describes the systematic changes of these level patterns with proton and neutron number by smooth variations of the model parameters $\beta A^{\frac{1}{3}}$, γ, and λ_F This goal will be achieved to large extent in the $A = 190$ mass region; for the $A = 135$ region, however, more experimental data are necessary to validate the two points. The present work is to be considered as a first step.

Quantitative agreement with experiment is not to be expected from the model as it stands now. This is because it does not account for some physical effects which are probably important for the nuclei considered. Two of these are:

(i) The β- and γ-fluctuations which lead to an overall compression of the energy spectrum and affect the transition probabilities. The compression of the experimental spectra as compared to the calculated ones is in fact observed in all cases discussed below.

(ii) The attenuation of the Coriolis interaction This effect is well known from strongly deformed odd-A nuclei and seems to play an important role also here in cases where the Fermi energy penetrates the j-shell level system. This point will be discussed in subsect. 3.2.4.

In addition, there are other, but possibly less important, effects related to the odd particle such as shifts of the core parameters β and γ, pair-blocking, mixing with other j-shells and with three or more quasiparticle configurations The relative uncertainty of how these different effects will change the results has motivated our choice for handling the free parameters. Thus we regard it as inadequate at the moment to make "best fits" to the experimental spectra, but rather choose to determine the model parameters from neighboring even nuclei as well as possible. The details of this procedure are described in sect. 2 The theoretical spectra, compared with experiment in sect. 3, then represent essentially parameter-free calculations.

In order to limit the size of this paper, no attempt is made to compare the calculated results with spectra of lighter nuclei and with non-unique parity states also The situation is more complex for non-unique parity states since there are usually several j-shells of the same parity near the Fermi energy which tend to mix with each other. A systematic comparison with a mixed j-shell calculation will be interesting, but has not been performed so far

2. Determination of the standard parameters

The goal is to determine the deformation parameter β and the asymmetry parameter γ from the lowest excited states of the adjacent even nuclei and to determine the

Fermi energy λ_F from a single-particle level scheme. Such a procedure is not unambiguous for several reasons:

(i) The low-energy spectra of even transitional nuclei differ in general from those of a perfect triaxial rotor, and there are different ways to adjust β and γ.

(ii) In a number of cases, the first excited energies of the even nuclei are rapidly changing with mass number so that the question arises which of the two neighbors or which average of them should be taken

(iii) Furthermore, there is evidence in some cases that the odd nucleon polarizes the core so that the parameters of the even neighbors are not quite applicable to the odd-A nucleus

Being aware of these ambiguities, a certain compromise has been chosen

The parameter γ is determined from the energy ratio of the second 2^+ state to the nearest member of the ground state band, in most cases the first 4^+ state For particle spectra (λ_F below j-shell), the $(A-1)$ neighbor is chosen as reference nucleus and, for hole spectra (λ_F above the j-shell), the $(A+1)$ neighbor. This procedure is well supported by the comparison with experiment. It can possibly be justified by stating that an odd-A spectrum should be compared with that even nucleus which has the same number of unbroken particle (or hole) pairs counting from the next closed shell. The energy ratios $E_{2_1^+}/E_{2_2^+}$, $E_{4_1^+}/E_{2_2^+}$ and $E_{6_1^+}/E_{2_2^+}$ are listed in table 1 for different

TABLE 1

Ratios of the first 2_1^+, 4_1^+, and 6_1^+ energies to the second 2_2^+ energy for a triaxial rotor with irrotational moments of inertia

γ (deg)	$E_{2_1^+}/E_{2_2^+}$	$E_{4_1^+}/E_{2_2^+}$	$E_{6_1^+}/E_{2_2^+}$	$E_{2_1^+}\Big/\left(\frac{6\hbar^2}{2\mathscr{I}_0}\right)$
10	0 062	0.208	0.434	1.06
11	0.076	0.253	0.527	1 08
12	0 092	0 305	0.632	1 09
13	0.108	0 357	0.738	1.11
14	0.126	0 415	0.854	1 13
15	0 146	0 476	0 973	1 15
16	0 167	0 543	1.10	1.17
17	0 186	0 603	1 25	1 19
18	0.214	0.685	1.40	1 21
19	0 239	0.758	1.54	1.24
20	0.267	0 838	1.60	1 27
21	0.296	0.910	1 73	1.30
22	0.326	0 982	1.86	1.33
23	0 357	1 05	1 98	1 36
24	0 387	1 12	2 11	1 39
25	0 417	1 18	2 22	1 42
26	0 445	1 23	2.32	1 45
27	0 466	1.27	2 39	1 47
28	0 482	1 30	2.44	1 48
29	0 495	1 32	2 48	1 49
30	0 500	1 33	2 50	1 50

γ-values over the range $10° \leqq \gamma \leqq 30°$. Since the energy spectrum of the even triaxial rotor is symmetric about $\gamma = 30°$ (see fig. 2 of I), this procedure cannot distinguish between prolate triaxial shapes $0° < \gamma < 30°$ and oblate triaxial shapes $30° < \gamma < 60°$. The information to which side a certain nucleus belongs has to be taken from the odd-A spectrum.

The parameter β is determined from the average $\bar{E}_{2^+} = \frac{1}{2}(E_{2^+}^{(A-1)} + E_{2^+}^{(A+1)})$ of the first 2^+ energies of the $(A-1)$ and the $(A+1)$ neighbor. Taking averages at this point seems to be inconsistent with the determination of γ; empirically, however, this rule yields good agreement for all the $h_{\frac{11}{2}}$ spectra considered below. The $h_{\frac{9}{2}}$ spectra seem to have larger β as will be discussed in subsects. 3.1.1 and 3.1.4. Equating the expression

$$E_{2^+}^{\mathrm{th}}(\gamma) = \frac{6\hbar^2}{2\mathscr{I}_0} \frac{9 - \sqrt{81 - 72 \sin^2 3\gamma}}{4 \sin^2 3\gamma}$$

for the first 2^+ energy of the even triaxial rotor with the experimental $\bar{E}_{2^+}$ and using the general relation $\hbar^2/2\mathscr{I}_0 = 204\ \mathrm{MeV}/\beta^2 A^{\frac{5}{3}}$ [see eq. (2.53) of I], one obtains

$$\beta = \left[\frac{1224}{A^{7/3}\bar{E}_{2^+}} X(\gamma)\right]^{\frac{1}{2}},$$

where $\bar{E}_{2^+}$ is taken in MeV. The γ-dependent factor

$$X(\gamma) = E_{2^+}^{\mathrm{th}}(\gamma)/6\hbar/2\mathscr{I}_0$$

is listed for convenience in column 5 of table 1 for different γ.

The position of the *Fermi energy* λ_F relative to the j-shell on which the unique parity states are built determines the particle or the hole character of the spectrum. For a given j-shell, λ_F is estimated from a Nilsson level scheme for $\gamma = 0°$, since a good general level scheme showing the single-particle energies as functions of β *and* γ has not been at our disposal†. This estimate is sufficient as long as λ_F is located outside the j-shell level system. In cases where λ_F penetrates the j-shell appreciably the fine adjustment of λ_F has been performed by fitting approximately the first $(j-1)$ state of the odd-A spectrum. In figs. 2–9, λ_F is given in the form $\tilde{\lambda}_F = (\lambda_F - \varepsilon_1)/(\varepsilon_2 - \varepsilon_1)$ for particle spectra and $\tilde{\lambda}_F = (\varepsilon_{(j+\frac{1}{2})} - \lambda_F)/(\varepsilon_{(j+\frac{1}{2})} - \varepsilon_{(j-\frac{1}{2})})$ for hole spectra where ε_ν with $\nu = 1, 2, \ldots j+\frac{1}{2}$ are the single-particle energies of the j-shell.

The parameters determined according to this procedure are called standard parameters. In the following comparison with experimental spectra, standard parameters are used unless stated differently.

3. Comparison with experiment

3.1 THE $A = 190$ MASS REGION

Considerable evidence for triaxial shapes is found from odd-A nuclei in the $A = 190$ mass region. The experimental systematics of odd-proton negative-parity states are

† Single-particle energies for $\beta = 0.3$ and $0° \leqq \gamma \leqq 60°$ are given in ref. [43]), for $0 < \beta < 0.6$ and $\gamma = 30°$ in ref. [31])

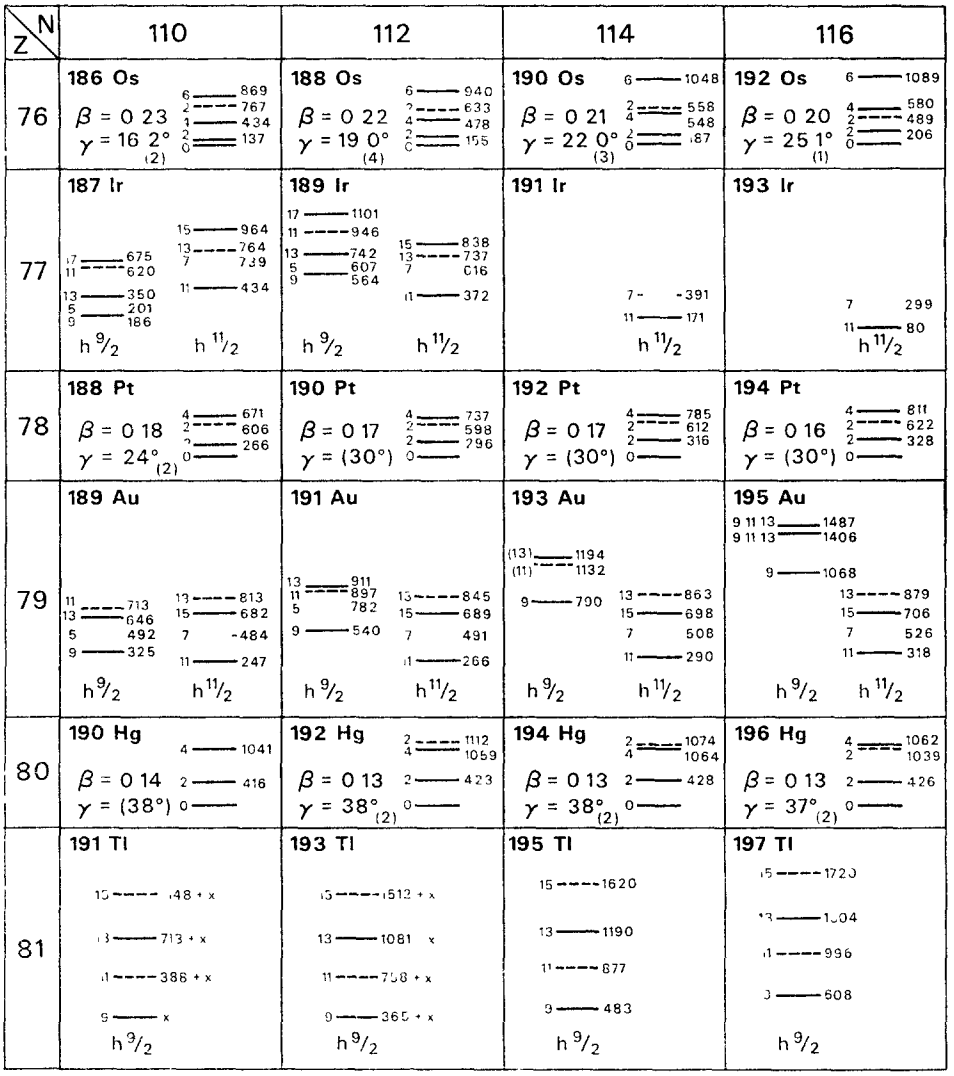

Fig 1. Systematics of unique-parity spectra built on the $h_{\frac{9}{2}}$ and the $h_{\frac{11}{2}}$ shell of odd-proton nuclei in the $A = 190$ mass region. Energies (in keV) of adjacent even nuclei [13]) and derived values for β and γ or estimates (in parentheses) are given Estimates of the uncertainty $\Delta\gamma$ are also shown in parentheses as changes in the last digit of the given γ-values. Spin values ($2I$) and energies (keV) of odd-A states are based on· ^{187}Ir, refs [2,3]), ^{189}Ir, refs. [2,4]); ^{191,193}Ir, refs [5,6]), ^{189}Au, ref [7]), ^{191}Au, ref [8]) and systematics, ^{193}Au, refs [9,16]); ^{195}Au, refs [9–11]), Tl isotopes, ref [12])

summarized in fig 1. The energy spectra represent either particle states built on the $h_{\frac{9}{2}}$ shell or hole states built on the $h_{\frac{11}{2}}$ shell. For comparison, lowest excited states of the even nuclei in this region and their parameters β and γ are also given in fig. 1 including estimates for the uncertainty in γ. The $\Delta\gamma$ values give the difference between the

standard γ-value and those derived from the other energy ratios given in table 1 whichever differs most. Only the Os spectra agree well enough with the rigid triaxial rotor spectrum to allow a γ-determination of better than 1°. The γ-values of the heavier Pt isotopes are almost $\gamma = 30°$, but is is unclear whether slightly below or slightly above this value. One finds a remarkable constancy of the parameters as a function of neutron number (less pronounced for Os isotopes), however a strong variation with proton number as it approaches $Z = 82$ The standard parameters vary from $\beta = 0\,23$ and $\gamma = 16°$ for ^{186}Os to $\beta = 0.13$ and $\gamma = 38°$ for the Hg isotopes

The variation of γ from shapes of prolate type ($0° < \gamma < 30°$) to shapes of oblate type ($30° < \gamma < 60°$) covers the interesting region where the theoretical odd-A spectra change from a decoupled level sequence ($j, j-2, j+2, j+1, \ldots$) to a strongly coupled level sequence ($j, j+1, j+2, \ldots$) for particle cases and vice versa for hole cases (compare fig. 6 and subsect. 3.2. of I). The theoretical expectation is nicely borne out by the experimental spectra, provided one associates the particle spectra with the $(A-1)$ even neighbor as core and the hole spectra with the $(A+1)$ even neighbor Doing this, one expects, e.g., for ^{187}Ir, a decoupled $h_{\frac{9}{2}}$ spectrum on the $\gamma = 16°$ core of ^{186}Os, but at the same time a strongly coupled $h_{\frac{11}{2}}$ spectrum built on a hole in the $\gamma = 24°$ core of ^{188}Pt. For ^{189}Au, the prolate-type ^{188}Pt now serves as a core for the $h_{\frac{9}{2}}$ spectrum, but the $h_{\frac{11}{2}}$ spectrum is built on the oblate-type ^{190}Hg with $\gamma \approx 38°$, and both spectra are expected to be of decoupled structure in good agreement with experiment. One can follow this line one step further to the Tl isotopes where now the $h_{\frac{9}{2}}$ particle spectra on the oblate-type Hg cores are of strongly coupled structure as expected. Note the remarkable constancy of the $h_{\frac{11}{2}}$ spectra in Au and the $h_{\frac{9}{2}}$ spectra in Tl for all isotopes which reflects the constancy of the Hg core energies. This survey already indicates that there is a continuous transition from the prolate side to the oblate side through the triaxial region It can be followed over a series of nuclei There is no sudden switch from $\gamma = 0°$ to $\gamma = 60°$

The characteristics of the different triaxial regions can be traced to much finer details of the experimental data as will be shown in the following for some representative nuclei. Examples are picked out for which the measured data are most complete and which cover the range from ^{199}Tl to ^{187}Ir Most evidence for triaxial shapes is obtained from the positions of unfavored yrast states and second and third states of the same spin, some of which form $\Delta I = 1$ bands beside the yrast band. These side bands are expected for triaxial odd-A rotors and will be discussed in connection with ^{187}Ir.

At the present time, there are much less data known for odd-neutron nuclei [14,15] than for odd-proton nuclei In the following collection, ^{193}Hg [ref. [15]] is included as one example for an $i_{\frac{13}{2}}$ neutron spectrum Also the experimental results on moments and transition probabilities are still rare, but the few data known, e g., for ^{187}Ir, agree well with the model calculation. The largest systematic discrepancy observed in the following examples concerns a general overall compression of the experimental spectra as compared with the calculated ones It should be mentioned that this

discrepancy cannot be removed neither by fitting the free parameters to the odd-A spectra nor by varying the parameters within the uncertainty of their determination. Since the compression is equally observed for the neighboring even nuclei, it is very likely to reflect a certain softness of the core wave functions which is not taken into account in the present rigid rotor description

3.1.1. The nucleus ^{199}Tl. The negative-parity states of Tl isotopes [12]) represent a strong case for the present model. The strongly coupled bands built on the $h_{\frac{9}{2}}$ proton shell closely follow the spectrum of a rigid triaxial odd-A rotor. This is shown for ^{199}Tl in fig 2. The theoretical spectrum is calculated with standard parameters except for β A value $\beta = 0.15$, instead of $\beta = 0.13$ from ^{198}Hg or the even smaller value of ^{200}Pb, gives much improved agreement between the theoretical and the experimental spectrum. The larger β-value indicates that the $h_{\frac{9}{2}}$ particle has a deforming effect on the ^{198}Hg core

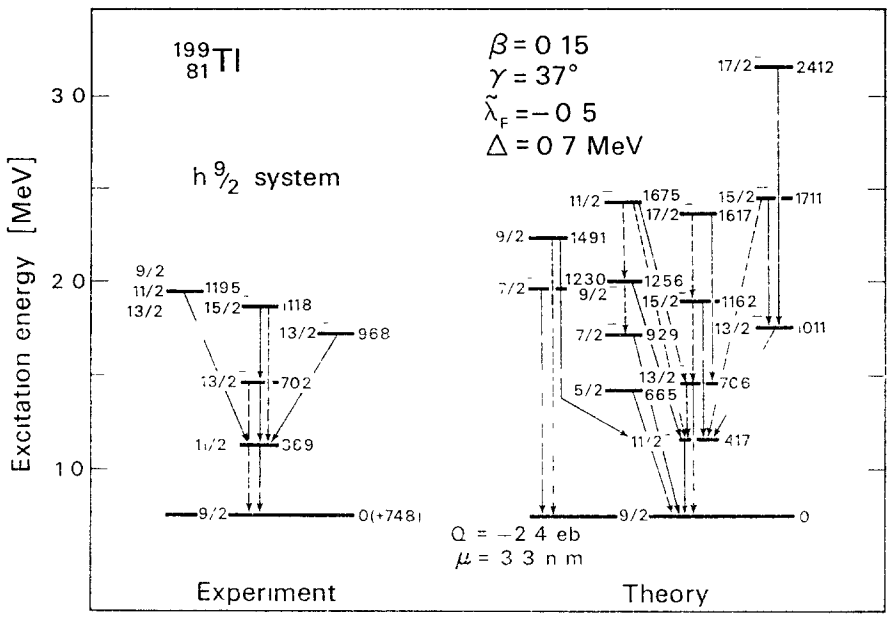

Fig 2 Negative-parity states in ^{199}Tl Solid lines indicate the strongest observed and calculated decay transitions of each level, broken lines all other transitions with intensities of at least 50 % of that of the strongest transition Energies are given in keV relative to the basic state The calculated quadrupole moment and magnetic moment of the basic state are also given

Strong evidence for a triaxial shape is provided by the second $\frac{13}{2}^-$ state As may be checked from fig. 6a in I, the energy of this state changes rapidly with γ relative to the ground band Here, its experimental position is well reproduced with the standard value $\gamma = 37°$ derived from the ^{198}Hg core Candidates for the $(\frac{13}{2}^-)_2$ state are also seen in ^{197}Tl and ^{195}Tl at about the same position. The 1195 keV state (relative energy) in ^{199}Tl can possibly be identified with the second $\frac{9}{2}^-$ model state. As does the

$(\frac{13}{2}^-)_2$ state, it decays most strongly to the first $\frac{11}{2}^-$ state in the measured as well as in the calculated spectrum. The detection of the $\frac{5}{2}^-$ state should be a challenge for experiment. It is predicted to lie just below the $(\frac{13}{2}^-)_1$ state and should decay *via* E2 to the $(\frac{9}{2}^-)_1$ state or *via* E1 to the $\frac{3}{2}^+$ state at 367 keV in ^{199}Tl. The $(\frac{13}{2}^-)_2$ state has the character of a $(\bar{K}-\bar{\Omega} = +2)$ γ-band head built on the $\frac{9}{2}^-$ ground state (see subsects. 3 4 and 3.5 of I) The $(\frac{9}{2}^-)_2$ state belongs to the corresponding low-spin band with $(\bar{K}-\bar{\Omega} = -2)$ character. It is interesting to note that the states of this band are most strongly decaying to the ground band rather than within the band. This band leaking will be further studied in examples that follow.

3 1 2. The nucleus ^{195}*Au* The $h_{\frac{11}{2}}$ spectra in Au isotopes [10]) are based on the same oblate Hg cores as the $h_{\frac{9}{2}}$ systems in the Tl isotopes, but since they represent hole states they have a decoupled level order In fig 3, the standard model calculation is compared with the $h_{\frac{11}{2}}$ level scheme of ^{195}Au. The numerous high-spin and low-spin states known from heavy-ion and decay experiments are all reproduced by the model calculation including the transition branchings. Again, the result is rather specific concerning the shape asymmetry For example, the near degeneracy of the first $\frac{9}{2}^-$ and $\frac{13}{2}^-$ states as well as the position of the unfavored $\frac{17}{2}^-$ yrast state just below the favored $\frac{19}{2}^-$ state and the near-crossing of the $(\frac{11}{2}^-)_2$ and $(\frac{11}{2}^-)_3$ states confine γ to within a few degrees about the standard Hg value $\gamma = 37°$ No comparable agreement would be obtained with an axially symmetric core

Some finer details should be pointed out As discussed in connection with fig. 5b in I, the second and third $\frac{11}{2}^-$ state exchange structure at a deformation $\beta \approx 0\ 15$, and one expects the transition probabilities in the decay of these states to vary

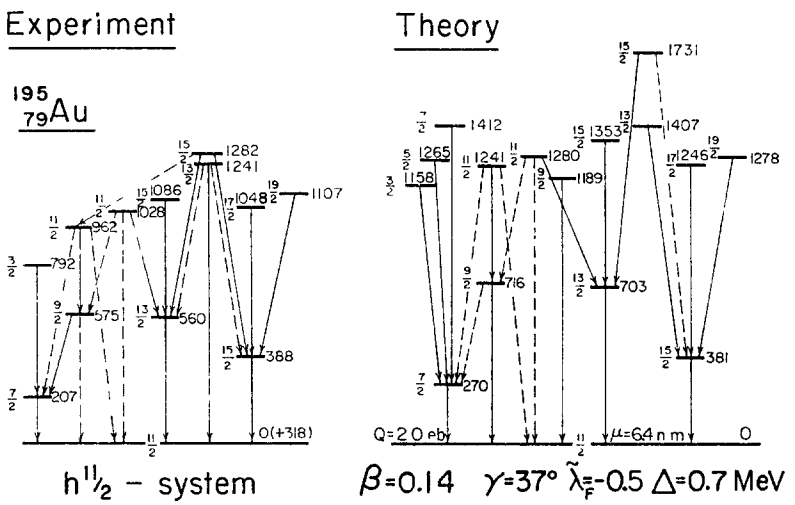

Fig 3 Negative-parity states in ^{195}Au Energies and moments are defined as in fig 2 Solid lines indicate transitions with 80 to 100 %, broken lines transitions with 20 to 80 % of the strongest decay intensity of each level Calculated intensities are based on calculated B(E2) and B(M1) values, but experimental transition energies when known

TABLE 2

Experimental and theoretical relative transition rates (in %) in the decay of the second and third $\frac{11}{2}^-$ state of ^{195}Au

I_i	E_i (keV)	→	I_f	E_f (keV)	Relative transition rates		
					exp [a])	theory	
						$\beta = 0\,144$	$\beta = 0.141$
$\frac{11}{2}$	962	→	$\frac{9}{2}$	575	52	57	4
			$\frac{13}{2}$	560	3	8	25
			$\frac{7}{2}$	207	11	15	11
			$\frac{11}{2}$	0	34	20	40
$\frac{11}{2}$	1028	→	$\frac{9}{2}$	575	34	33	39
			$\frac{13}{2}$	560	49	38	35
			$\frac{7}{2}$	207		1	2
			$\frac{11}{2}$	0	17	28	24

Experimental energies relative to the first $\frac{11}{2}^-$ state identify the states
[a]) Ref [9])

strongly with β. In table 2, relative transition intensities measured in ^{195}Au are compared with calculated ones Fair agreement is obtained with a value $\beta = 0\,144$ slightly larger than the standard value $\beta = 0.141$. Energies and transition lines for ^{195}Au in fig. 5 are based on the calculation with $\beta = 0\,144$ Concerning the very sharp change with $\beta A^{\frac{1}{3}}$ in the decay of the second $\frac{11}{2}$ state as shown in table 2, a recent systematic study on the Au isotopes [44]) seems to show that this effect is indeed present in experiment when going from ^{195}Au to ^{189}Au.

Three more negative-parity states than shown in fig. 3 have been found for ^{195}Au in a recent decay study [11]), a $\frac{9}{2}^-$ state at 1068 keV and two $(\frac{9}{2}, \frac{11}{2}, \frac{13}{2})^-$ states at 1406 and 1487 keV. The calculation yields a second $\frac{9}{2}^-$ state, but no more $\frac{9}{2}^-$, $\frac{11}{2}^-$, or $\frac{13}{2}^-$ states in this region. Considering the decay of the additional states to their $\frac{9}{2}^-$ member and then most strongly to a $\frac{7}{2}^+$ state, one is tempted to attribute them to an $h_{\frac{9}{2}}$ system with a basic $\frac{9}{2}^-$ state and, depending thereon, an $\frac{11}{2}^-$ and a $\frac{13}{2}^-$ state, in analogy to the first $\frac{13}{2}^-$ and $\frac{15}{2}^-$ levels of the $h_{\frac{11}{2}}$ system. Provided this interpretation is right, the calculation accounts for all measured negative-parity states in ^{195}Au The $h_{\frac{9}{2}}$ system has been observed beside the $h_{\frac{11}{2}}$ system in ^{189}Au [ref. [7])], ^{193}Au [ref. [16])], ^{187}Ir [ref. [2])] and ^{189}Ir [ref. [2])]. It can also be identified in ^{191}Au [ref. [8])].

3.1.3. The nucleus ^{193}Hg. In fig. 4, the measured ^{193}Hg spectrum [15]) (low-energy part < 1 5 MeV) built on an $i_{\frac{13}{2}}$ neutron hole is compared with the model calculation. The decoupled level order of the yrast band with the favored $\frac{13}{2}^+$, $\frac{17}{2}^+$, $\frac{21}{2}^+$, $\frac{25}{2}^+$ states and the unfavored $\frac{15}{2}^+$ and $\frac{19}{2}^+$ states is reproduced by both calculations for $\gamma = 38°$ and $\gamma = 60°$. This again confirms an oblate type shape for Hg isotopes. Evidence for triaxiality is given by the second $\frac{19}{2}^-$ state which has been observed in experiment, though with an uncertainty concerning the parity. The relative independ-

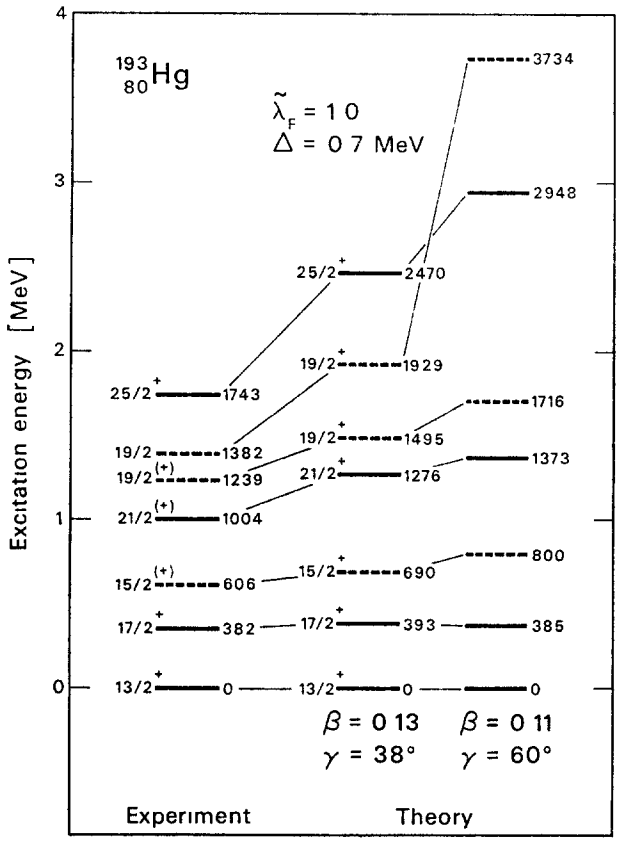

Fig. 4. Positive-parity states in ^{193}Hg.

ence of γ seen for *all* calculated yrast states is partly due to the Fermi energy which lies inside the $i_{\frac{13}{2}}$ shell for ^{193}Hg. There is a sharper variation of the unfavored states with γ, marking the triaxial region, in cases where λ_F is located outside the j-shell [see e.g., ^{195}Au in ref. [17])].

3.1.4. The nucleus ^{187}Ir ($h_{\frac{9}{2}}$ system). Extensive data have been obtained recently for ^{187}Ir and ^{189}Ir [ref. [2])]. The spectra of the two nuclei look very similar. Beside positive-parity bands built on the $s_{\frac{1}{2}}$ and $d_{\frac{3}{2}}$ shell, two separate negative-parity families are observed and attributed to the $h_{\frac{9}{2}}$ and $h_{\frac{11}{2}}$ shell. The $h_{\frac{9}{2}}$ system has a decoupled and the $h_{\frac{11}{2}}$ system a strongly coupled level order consistent with a prolate-type core. As seen in fig. 1, the adjacent even nuclei, e.g., of ^{187}Ir, possess quite different core parameters for ^{186}Os, $\beta = 0.23$ and $\gamma = 16°$ and, for ^{188}Pt, $\beta = 0.18$ and $\gamma = 24°$. Comparing the ^{187}Ir data with the model calculation in figs. 5 and 6, good agreement is found when using the ^{186}Os parameters for the $h_{\frac{9}{2}}$ particle spectrum and the ^{188}Pt value $\gamma = 24°$ and an averaged $\beta = 0.21$ (standard procedure) for the $h_{\frac{11}{2}}$ hole spectrum. This result indicates that a kind of shape isomerism exists in ^{187}Ir and also in ^{189}Ir. It is also present in the Au isotopes

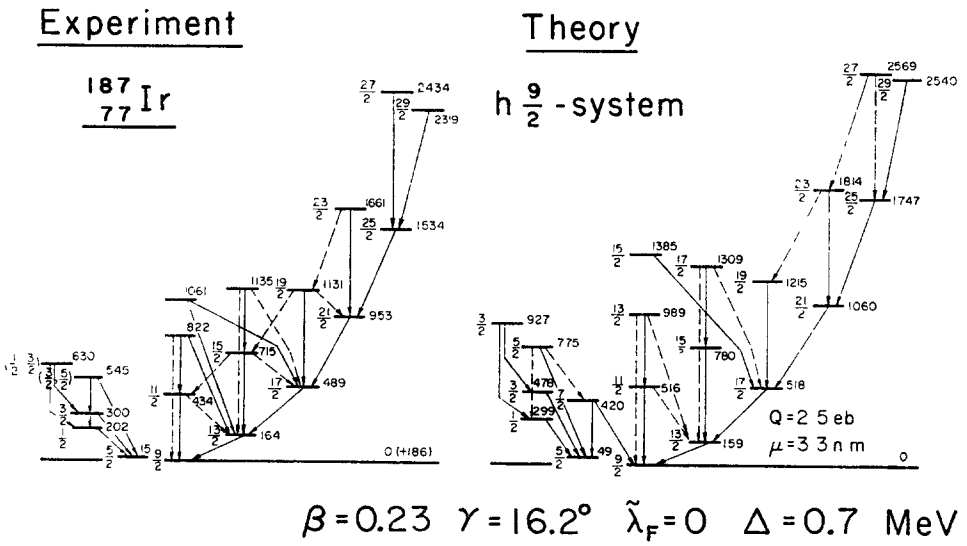

Fig 5. The $h_{\frac{9}{2}}$ family of negative-parity states in ^{187}Ir. Energies and moments are defined as in fig 2 Calculated transition lines are defined as in fig 3, experimental ones are solid for the strongest transition and broken for weaker transitions.

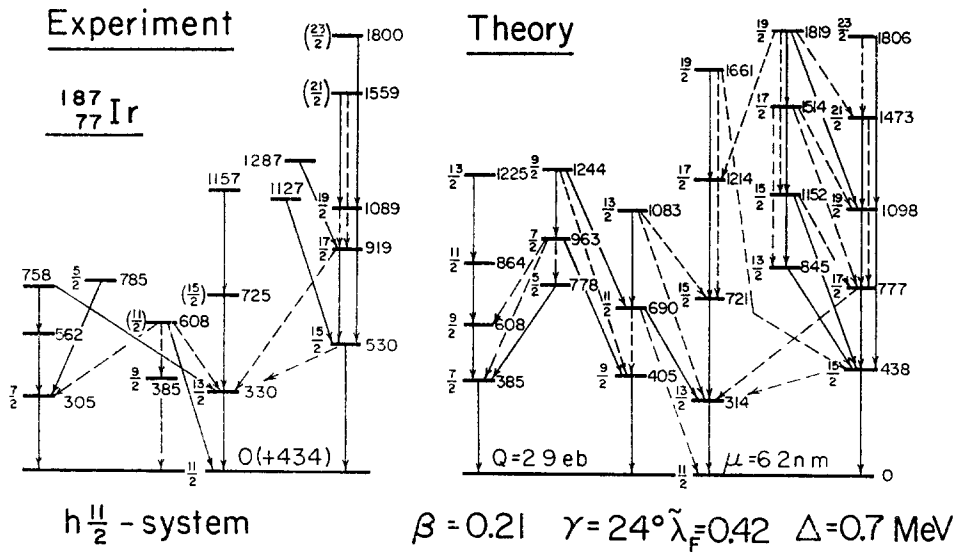

Fig 6 The $h_{\frac{11}{2}}$ family of negative-parity states in ^{187}Ir. For more details see fig 5.

In figs 5 and 6, the calculated levels have been ordered according to the $(\bar{K}, \bar{\Omega})$ classification discussed in I. Each column corresponds to an approximate $\bar{K}$ and $\bar{\Omega}$ value The experimental states have tentatively been arranged in the same order on the basis of their energies and their decay transitions An almost complete identification

of the experimental levels seems to be possible within the present model. In particular, a number of unassigned levels can be understood as higher members of the $\Delta I = 1$ vertical band structure.

For the $h_{\frac{9}{2}}$ system, shown in fig. 5, a large number of favored and unfavored yrast states and five non-yrast states have been observed. Their relative order is almost completely reproduced by the calculation. The result again sensitively depends on the shape asymmetry and confirms the value $\gamma = 16°$ derived from the ^{186}Os core. The triaxial coupling scheme, discussed in I, classifies the favored yrast states as approximate $\bar{K} = \bar{\Omega}, \bar{\Omega}+2, \bar{\Omega}+4, \ldots$ states with $\bar{\Omega} = \frac{9}{2}$. On the low-spin side, the yrast line is continued by approximate $\bar{K} = \bar{\Omega}-2, \bar{\Omega}-4, \bar{\Omega}-6$ states. Within the theoretical picture, the states on the yrast line mainly arise from collective rotation about the intrinsic $\hat{\mathbf{2}}$-axis, whereas the states that build up on each yrast state are related to an additional rotation about the intrinsic $\hat{\mathbf{1}}$-axis. The possibility of simultaneous rotation about two different intrinsic axes is a direct consequence of the triaxility of the core

The vertical band structure is expected to exist only for a few lowest states. In the $h_{\frac{9}{2}}$ spectrum of ^{187}Ir, the states with relative energies 0 keV ($\frac{9}{2}$), 434 keV ($\frac{11}{2}$), 822 keV may be understood in this way as a $\bar{K} = \bar{\Omega} = \frac{9}{2}$ band, and the states with energies 164 keV ($\frac{13}{2}$), 715 keV ($\frac{15}{2}$), 1135 keV as a $\bar{K} = \bar{\Omega}+2 = \frac{13}{2}$ band. The calculation suggests that higher states associated with this band structure predominantly decay to neighboring bands, in particular to yrast states. In fig. 5, this is seen for the $\frac{15}{2}^-$ model state at 1385 keV. Its strong decay to the $\frac{17}{2}^-$ yrast state suggests that it might correspond to the measured 1061 keV state. On the basis of the triaxial model, one would therefore assign the experimental states at 822, 1061, and 1135 keV (relative energy) as second $\frac{13}{2}^-$, $\frac{15}{2}^-$, and $\frac{17}{2}^-$ states, respectively. There are more high-spin model states below 1.4 MeV, not shown in fig. 6: two $\frac{9}{2}^-$ states at 829 and 1070 keV, two $\frac{11}{2}^-$ states at 1082 and 1377 keV, and another $\frac{13}{2}^-$ state at 1306 keV. Their calculated decays, however, agree much less or not at all with the decay pattern of the unassigned experimental levels.

3.1 5. The nucleus ^{187}Ir ($h_{\frac{11}{2}}$) system. The $h_{\frac{11}{2}}$ spectrum of ^{187}Ir is compared with the calculation in fig. 6. Energies and transition probabilities of this spectrum and of corresponding levels in heavier Ir isotopes strongly support the triaxial model An interpretation assuming an axially symmetric core must fail On the one hand, the low-lying $\frac{7}{2}^-$ state and its strongly enhanced $B(\mathrm{E2}; \frac{7}{2}^- \rightarrow \frac{11}{2}^-) = 0.3\ (e \cdot \mathrm{b})^2$, measured for ^{189}Ir [ref. [4])], could only be understood assuming an oblate core. On the other hand, the strongly coupled level order of the yrast band gives a clear indication for a prolate core. The suspicion of shape asymmetry in odd-A Ir isotopes has been raised in the past [6]) and is substantiated by the present work

The triaxial model calculation, using standard parameters, yields a low-lying $\frac{7}{2}^-$ state with a calculated $B(\mathrm{E2}; \frac{7}{2}^- \rightarrow \frac{11}{2}^-) = 0\,31\ (e \cdot \mathrm{b})^2$ simultaneously with the strongly coupled yrast band. In addition, it reproduces and elucidates the fairly complex level structure seen beside the yrast band and tentatively identifies five unassigned experimental states. It also provides good agreement between calculated

and measured B(E2) branching ratios and mixing ratios which are compared in tables 3a and 3b.

Some further comments should be made with respect to fig 6. The bands of the calculated spectrum are classified from left to right as ($\bar{K} = \frac{7}{2}$, $\bar{\Omega} = \frac{11}{2}$), ($\bar{K} = \frac{5}{2}$ $\bar{\Omega} = \frac{9}{2}$), ($\bar{K} = \bar{\Omega} = \frac{9}{2}$), ($\bar{K} = \bar{\Omega} = \frac{11}{2}$), ($\bar{K} = \frac{13}{2}$, $\bar{\Omega} = \frac{9}{2}$), and ($\bar{K} = \frac{15}{2}$, $\bar{\Omega} = \frac{11}{2}$) bands. They are related to $\frac{11}{2}$[505] and $\frac{9}{2}$[514] Nilsson bands and the corresponding

TABLE 3a

Comparison of experimental and theoretical B(E2) branching ratios within the $h_{\frac{11}{2}}$ system of ^{187}Ir

Transitions	B(E2) ratios	
	exp [a])	theory
$\frac{(\frac{15}{2})_1 \rightarrow (\frac{11}{2})_1}{(\frac{15}{2})_1 \rightarrow (\frac{13}{2})_1}$	$1.7^{+\infty}_{-1\,4}$	7 07
$\frac{(\frac{17}{2})_1 \rightarrow (\frac{13}{2})_1}{(\frac{17}{2})_1 \rightarrow (\frac{15}{2})_1}$	$0\,8^{+0\,2}_{-0\,6}$	0 86
$\frac{(\frac{15}{2})_2 \rightarrow (\frac{11}{2})_1}{(\frac{15}{2})_2 \rightarrow (\frac{13}{2})_1}$	$< 0\,1$	0 02
$\frac{(\frac{19}{2})_1 \rightarrow (\frac{15}{2})_1}{(\frac{19}{2})_1 \rightarrow (\frac{15}{2})_2}$	$1\,3^{+3\,1}_{-0\,6}$	1 37

[a]) Ref [2])

TABLE 3b

Comparison of experimental and theoretical mixing ratios δ(E2/M1) within the $h_{\frac{11}{2}}$ system of ^{187}Ir

Transition	E_γ (keV)	δ(E2/M1)	
		exp [a])	theory
$(\frac{13}{2})_1 \rightarrow (\frac{13}{2})_1$	200	$0\,0 < \delta < 0\,25$	0 04
$(\frac{13}{2})_1 \rightarrow (\frac{11}{2})_1$	330	$0\,25 < \delta < 0\,40$	0 18
$(\frac{17}{2})_1 \rightarrow (\frac{15}{2})_1$	389	$0\,15 < \delta < 0\,25$	0 19
$(\frac{17}{2})_2 \rightarrow (\frac{13}{2})_1$	395	$0\,28 < \delta$	0 21
$(\frac{9}{2})_1 \rightarrow (\frac{11}{2})_1$	385	$-0\,40 < \delta < -0\,15$	$-0\,14$

Measured transition energies have been used for calculating δ(E2/M1)
[a]) Ref [2])

low- and high-spin γ-bands. One should keep in mind, however, that these bands are strongly mixed and that the ($\bar{K}$, $\bar{\Omega}$) character is weakly defined in general (compare discussion in I). Though of rotational character, their band structure is often difficult to recognize experimentally since transitions within these bands are sometimes weaker than those to neighboring bands, in particular the yrast band For example, the measured 1127 keV state decaying to the $\frac{15}{2}^-$ yrast state is likely to be the $\frac{15}{2}$ member of the $\bar{K} = \frac{13}{2}$ band both because of its energy and its decay. The classifica-

tion of the measured 1287 keV state is unclear, though it might correspond to the $\frac{17}{2}^-$ state of the same band.

Some finer details of the $h_{\frac{9}{2}}$ spectrum in ^{187}Ir are not reproduced by the calculation. For example, the staggering of the experimental yrast band is not obtained. The general model solution contains yrast bands of this type as may be checked in fig 8 where the $h_{\frac{9}{2}}$ spectrum of ^{137}Nd and the corresponding calculation is shown, but it is not possible to reach this solution within the parameter uncertainty of ^{187}Ir. As a second point, the calculation yields the $\frac{7}{2}^-$ band too high relative to the $\frac{11}{2}^-$ band and the $\frac{15}{2}^-$ yrast state too low. Both points could be removed by changing γ within the uncertainty $\Delta\gamma = 2°$, but going with γ into opposite directions. This might indicate different γ-values within the same $h_{\frac{9}{2}}$ level system The ^{187}Ir result suggests that the Pt core on which the $h_{\frac{9}{2}}$ spectrum in ^{187}Ir is based is more γ-soft than, e g , the Hg cores on which the $h_{\frac{9}{2}}$ spectra in Au and the $h_{\frac{9}{2}}$ spectra on Tl are built

3.2. THE $A = 135$ MASS REGION

In the region with $Z > 50$ and $N > 82$, which was discovered as a new region of deformation a decade ago [18]), even nuclei consistently show a low-lying second 2^+ state at about the energy of the first 4^+ state This suggests that shape asymmetry might be important. First excited 0^+ states appear well separated at higher energies and exclude a two-phonon interpretation. Parameters β and γ of some even nuclei in this region are derived according to the standard procedure and are listed together with the lowest excitation energies in table 4. Estimates for the γ-uncertainty are also given. It is noted that most even-A spectra in this region follow the rigid-triaxial-rotor

TABLE 4

Lowest excitation energies in the $A = 135$ mass region [13]) and derived parameters

Isotope	Z	N	$E_{2_1^+}$	$E_{4_1^+}$	$E_{2_2^+}$	β	$\gamma(\Delta\gamma)$ (deg)	$\beta A^{\frac{1}{3}}$
^{128}Xe	54	74	443	1033	970	0 213	23(3)	5.4
^{130}Xe	54	76	536	1204	1122	0 190	23(4)	4 9
^{132}Xe	54	78	668	1440	1298	0.169	24(6)	4 4
^{130}Ba	56	74	357	902	908	0 231	22(2)	5 9
^{132}Ba	56	76	465	1128	1032	0 203	24(3)	5 3
^{134}Ba	56	78	605	1401	1168	0 177	25(5)	4 6
^{132}Ce	58	74	325	858		0 240		6 2
^{134}Ce	58	76	409	1049	966	0.210	23(2)	5 5
^{136}Ce	58	78	553	1316	1093	0 182	25(5)	4 8
^{134}Nd	60	74	294	789		0 256		6 7
^{136}Nd	60	76	374	974		0.223		5 9
^{138}Nd	60	78	521	1250	1014	0 185	26(4)	4 9

spacings much less than in the $A = 190$ region, probably due to larger β- and γ-softness. Considerable variations of β with mass number are found, whereas the γ-values are fairly constant in the range $20° < \gamma < 30°$. Decoupled odd-A spectra built on $h_{\frac{11}{2}}$ proton particles as well as strongly coupled spectra built on $h_{\frac{11}{2}}$ neutron holes are observed in this mass region and clearly indicate prolate-type shapes. Oblate shapes have been assumed in the past [19,20]), but they are ruled out also by recent measurement of quadrupole moments in even Ba isotopes [21]).

The exciting point about odd-A spectra and, in particular, families of unique-parity states is that they give more information about the shapes than just a classification as prolate or oblate; they allow to determine the shape asymmetry rather sensitively. Although the available experimental material on odd-A nuclei in the $A = 135$ mass region is still less abundant than for $A \approx 190$ nuclei, there already exists considerable

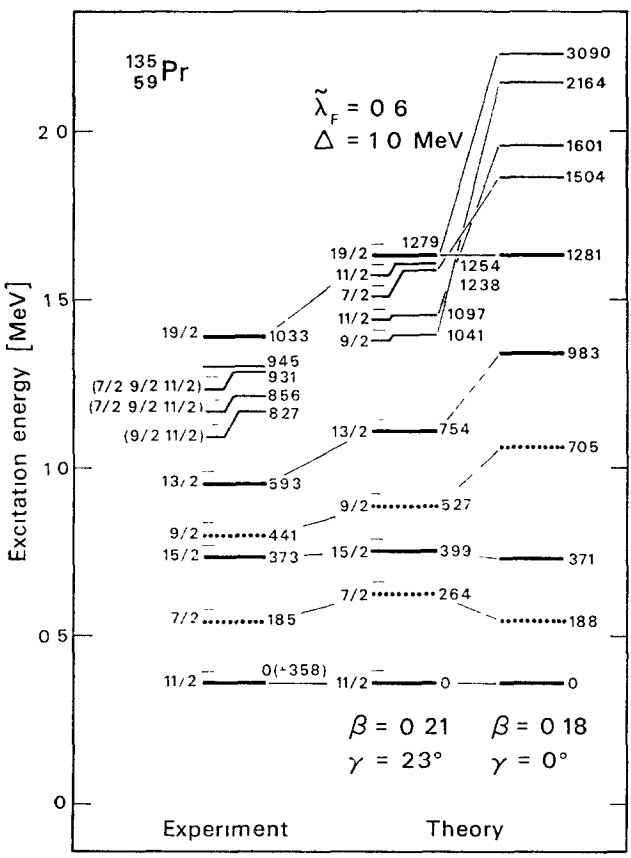

Fig. 7. Negative-parity states in ^{135}Pr below the $\frac{19}{2}^-$ state

evidence that the new region of deformation is mainly a triaxially deformed region - at least around $A = 135$. This conclusion is based

(i) on $h_{\frac{11}{2}}$ proton spectra observed in ^{133}La [refs. [22-24])], ^{135}La [ref. [24])], ^{135}Pr [ref. [25])] and ^{129}Cs [ref. [24])];

(ii) on yrast bands built on an $h_{\frac{11}{2}}$ neutron hole in ^{135,137}Nd [ref. [26])], ^{133,135}Ce [ref. [26])] and ^{131}Ba [ref. [27])] and on the decay spectrum of ^{137}Pr to ^{137}Nd [ref. [28])] and

(iii) on a recent lifetime measurement of favored yrast states in ^{129,131}La [ref. [29])]. Part of this evidence is discussed in the following.

3.2 1. The nucleus ^{135}Pr. The $h_{\frac{11}{2}}$ odd-proton spectra in the $A = 135$ mass region can be considered as the particle analogues of the $h_{\frac{11}{2}}$ hole spectra in the Au isotopes. For the Au isotopes, one has $\gamma \approx 37°$, and the Fermi energy lies above the $h_{\frac{11}{2}}$ shell, $\lambda_F > \varepsilon_{\frac{11}{2}}$; for La and Pr isotopes, one has $\gamma \approx 23°$ $(= 60° - 37°)$ and $\lambda_F > \varepsilon_{\frac{11}{2}}$. Due to the particle-hole symmetry (compare I), the corresponding $h_{\frac{11}{2}}$ spectra look very similar.

In fig. 7, this is demonstrated for ^{135}Pr, one of the rare cases in this region where both high-spin and low-spin data are available [25]). Beside the standard triaxial calculation with $\gamma = 23°$, the model solution for $\gamma = 0°$ is also shown for comparison. The effect of the triaxiality of the core is most evident for the group of second and third states with spin $\frac{7}{2}^-$, $\frac{9}{2}^-$, $\frac{11}{2}^-$ just below the $\frac{19}{2}^-$ yrast state. Possible theoretical partners for the experimental states are found in this energy region in the triaxial calculation, but lie far too high in energy for an axially symmetric core This strongly supports the assumption of shape asymmetry in ^{135}Pr. Concerning transition-branching ratios, experiment and theory do not compare well enough to identify these states separately. For this reason, they are not reported here.

The standard calculation yields more states in the region around the $\frac{19}{2}^-$ state. a $\frac{5}{2}^-$ state at 1279 keV, a $\frac{13}{2}^-$ state at 1456 keV, a $\frac{3}{2}^-$ state at 1517 keV, a $\frac{15}{2}^-$ state at 1700 keV, and a $\frac{17}{2}^-$ state at 1746 keV. Since the ^{135}Pr spectrum is fed by decay from a $\frac{9}{2}^-$ state in ^{135}Nd with all log ft values < 7, these states are probably not populated. The $\frac{5}{2}^-$ state has been observed near the expected energy in ^{133}La for which a spectrum similar to that of ^{135}Pr has been found [23,24])

3 2.2 The nuclei ^{129}La and ^{131}La Transition probabilities provide another sensitive test for shape asymmetry Here, we discuss E2 transitions between favored yrast states in decoupled bands. Although the favored energies do not strongly depend on γ, the B(E2) values do as shown in fig. 9 of I For example, the calculated ratio $R = B(\mathrm{E2}; (J+2) \to J)/B(\mathrm{E2}; 2^+ \to 0^+)_{\mathrm{av}}$ drops from values $R \approx 1\,5$ for axially symmetric shapes at $\gamma = 0°$ to values $R \approx 1.2$ for $\gamma = 20°$ and $R \approx 0.9$ for $\gamma = 25°$. The ratios R also depend slightly on $\beta A^{\frac{1}{3}}$ and λ_F. Recent experiments seem to confirm the theoretical result. For the decoupled $i_{\frac{13}{2}}$ bands in the axially symmetric nuclei ^{157,159}Er (region of high-lying second 2^+ states!) R-values even somewhat larger than 1 5 were obtained [30]), whereas values around 1.2 are found for the decoupled $h_{\frac{11}{2}}$ spectra in ^{129,131}La, indicating triaxiality of the cores [29]).

The results for ^{129}La and ^{131}La are shown in table 5. The experimental numbers agree with the triaxial model calculation, confirming $\gamma = 22°$ derived from ^{130}Ba

TABLE 5

Measured and calculated $B(E2)$ values for ^{129}La and ^{131}La.

$B(E2)\downarrow(e^2\ b^2)$	^{129}La	^{131}La
$\frac{15}{2}^- \rightarrow \frac{11}{2}^-$	$E_\gamma = 269$ keV	$E_\gamma = 336$ keV
Experiment [a])	0 42±0 02	0 34±0 02
Theory γ_{exp}	0 37±0 02 [b])	0 32±0.02 [c])
Theory $\gamma = 0°$	0 50	0.45
$\frac{19}{2}^- \rightarrow \frac{15}{2}^-$	$E_\gamma = 475$ keV	$E_\gamma = 533$ keV
Experiment [a])	0 38±0.06	0 33±0.03
Theory γ_{exp}	0 42±0 02 [b])	0.37±0 02 [c])
Theory $\gamma = 0°$	0 52	0 47
$B(E2, 2^+ \rightarrow 0^+)_{av}$ [a])	0 33±0 05	0 28±0 07

The parameter $\beta A^{\frac{1}{3}}$ has been determined from the experimental average $B(E2; 2^+ \rightarrow 0^+)_{av}$ of the adjacent even nuclei. The given theoretical errors are due to the uncertainty in γ_{exp}

[a]) Ref [29])

[b]) Parameters used: $\beta A^{\frac{1}{3}} = 6\ 8$, $\gamma_{exp} = (22\pm2)°$, $\tilde{\lambda}_F = 0\ 5$, $\Delta = 1\ 0$ MeV

[c]) Parameters used: $\beta A^{\frac{1}{3}} = 6\ 4$, $\gamma_{exp} = (23\pm2)°$, $\tilde{\lambda}_F = 0\ 5$, $\Delta = 1\ 0$ MeV

within an uncertainty of about $\pm 3°$. Values calculated with $\gamma = 0°$ are significantly too large. The $B(E2)$ values for both the $\frac{15}{2}^- \rightarrow \frac{11}{2}^-$ and the $\frac{19}{2}^- \rightarrow \frac{15}{2}^-$ transitions have been measured and are found very close to each other. This is an interesting result since it probably rules out a weak-coupling interpretation. The experimental ratios $B(E2; \frac{19}{2} \rightarrow \frac{15}{2})/B(E2; \frac{15}{2} \rightarrow \frac{11}{2})$ are slightly smaller than one, whereas weak coupling would give approximately 1.4 for a rigidly rotating core (almost independently of γ) or even 2.0 assuming the core to be a harmonic vibrator.

It should be further mentioned that the next higher yrast transition $(J+6) \rightarrow (J+4)$ is expected to behave differently from the $(J+4) \rightarrow (J+2)$ transition according to the triaxial model. As shown in ref. [29]), the calculated ratio $B(E2; \frac{23}{2} \rightarrow \frac{19}{2})/B(E2, \frac{19}{2} \rightarrow \frac{15}{2})$ increases rapidly beyond $\gamma = 20°$ and becomes larger than 2 in the region $30° < \gamma < 40°$. At the moment, it is an open question whether also this feature of the present model can be confirmed.

3.2.3 The nucleus ^{137}Nd Combined data for ^{137}Nd, obtained from heavy-ion and β-decay experiments [26, 28]), are compared with theory in fig. 8 With 77 neutrons ^{137}Nd is the neutron analogue of ^{187}Ir which has 77 protons. As seen from the comparison of fig 6 and fig. 8, the $h_{\frac{11}{2}}$ spectra of both nuclei – at least their high-spin part – are remarkably similar. As in ^{187}Ir, a strongly coupled, heavily distorted yrast band is observed in ^{137}Nd and indicates a triaxial shape It is well reproduced by the calculation with standard parameters and confirms γ to lie within a few degrees about the standard value $\gamma = 26°$, derived from ^{138}Nd. In fact, the narrow spacing between the $(\frac{13}{2}^-)_1$ and $(\frac{15}{2}^-)_1$ states points to a slightly larger γ.

There is an additional group of negative-parity levels observed in ^{137}Nd as shown on the left-hand side of fig. 8 Concerning these levels, no definite conclusion can be

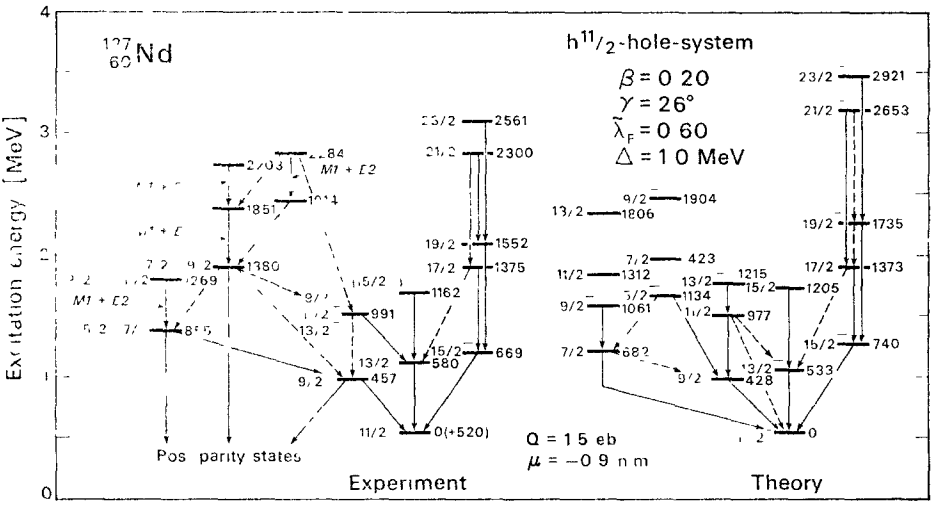

Fig 8 Negative-parity states in ^{137}Nd Energies and moments are defined as in fig. 2, transition lines as in fig 3. Not all theoretical transitions are shown

drawn at the moment One could think of the 855 keV state (1374 keV absolute energy) as the $(\frac{7}{2}^-)_1$ model state. On this assumption, however, it should strongly decay to the basic $\frac{11}{2}$ state (78 % theoretical branching) and much less to the $(\frac{9}{2}^-)_1$ state. Another possiblity would be to identify the 855 keV state as the $(\frac{5}{2}^-)_1$ model state, although this would mean a large discrepancy in energy. Both possibilities are not very convincing. The experimental level system built on the 1380 keV state (1899 keV absolute energy) is even more difficult to understand within the $h_{\frac{11}{2}}$ model spectrum, since the potential partners among the model states in this region predominantly decay to the $K = \Omega = \frac{9}{2}$ and $K = \Omega = \frac{11}{2}$ bands and not to their next neighbors as in experiment. Our conclusion, therefore, is that these states are *not* likely to be based on the $h_{\frac{11}{2}}$ shell. An alternative would be to attribute them to the $f_{\frac{7}{2}}$ and possibly the $h_{\frac{9}{2}}$ neutron shell. More experimental results are necessary to check this question.

3 2 4. The nucleus ^{133}*Ce.* The $N = 75$ isotones ^{135}Nd, ^{133}Ce, and ^{131}Ba exhibit almost identical negative parity spectra [26,27]). The case ^{133}Ce is presented in fig. 9. Again, the experimental spectrum is much better reproduced by the standard triaxial calculation than by the $\gamma = 0°$ solution. A discrepancy, however, remains for the lowest $\frac{9}{2}$ state. Although the penetration of the Fermi energy into the $h_{\frac{11}{2}}$ shell brings the $\frac{9}{2}$ state down, it is not lowered far enough This difficulty with $I < j$ states is known from Coriolis distorted bands in strongly axially deformed nuclei and is usually remedied by an *ad hoc* attenuation of the Coriolis matrix elements. No such procedure has been adopted in this work, since it would obscure the clear physical outlines of the present model A physical explanation of this effect has been given recently by Ring and Mang [32]), based on a self-consistent treatment of the core

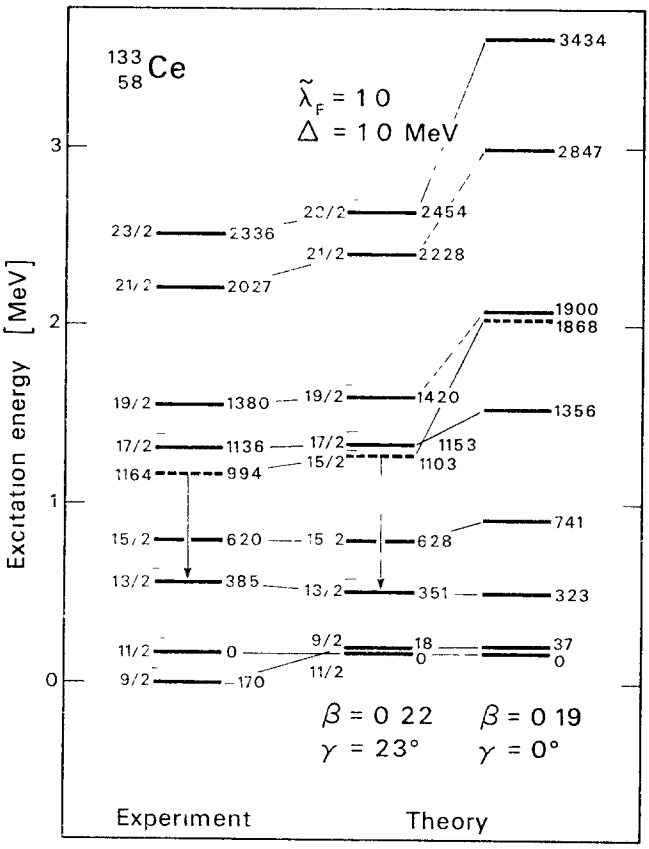

Fig 9 Negative-parity states in ^{133}Ce

moment of inertia It is still an open question how to incorporate their treatment into a triaxial-rotor model where one has three rotation axes rather than one.

4. Discussion of results and relations to other models

It has been shown that the predictions of the triaxial-rotor-plus-quasiparticle model are in remarkable agreement with a number of unique-parity spectra of odd-A transitional nuclei. It describes the nucleus ^{199}Tl at the border to the closed-shell Pb region as well as ^{187}Ir which borders strongly deformed rare-earth nuclei. It also seems to apply to the $50 < Z, N < 82$ nuclei though more experimental data are needed to confirm its validity in that region How is this success of a rigid-triaxial-rotor model to be interpreted? It would be naive to take the rigid shape literally There is much evidence that these transitional nuclei have fairly soft, fluctuating shapes The question is rather *to which extent* these nuclei are soft or rigid and what

one can learn about it from the present result. In what follows, a qualitative answer is given.

Assuming that the collective motion of low-excited nuclei is dominated by the quadrupole degrees of freedom, the nuclear softness is most conveniently discussed in terms of potential-energy surfaces (PES) in the (β, γ) plane. Fig 10 displays some typical situations in a schematic way.

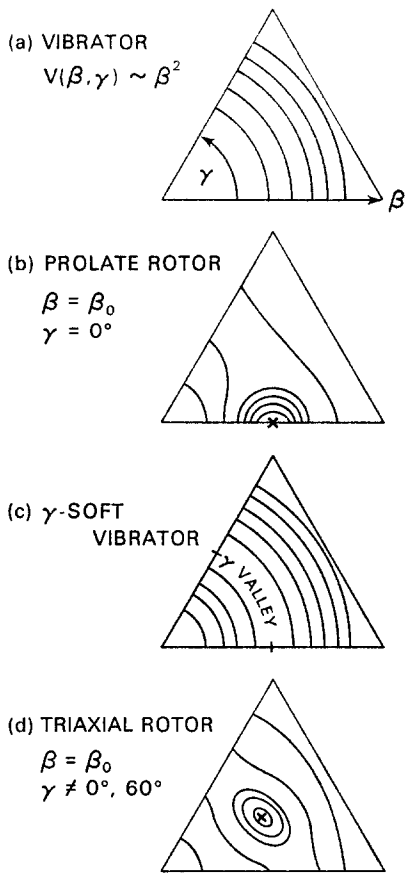

Fig 10 Schematic potential-energy surfaces for different types of nuclei

(i) Fig. 10a: The harmonic-vibrator PES which only occurs for closed-shell nuclei and their next neighbors.

(ii) Fig. 10b: The prolate-rotor PES with a deep potential minimum at $\beta_0 \neq 0$ and $\gamma_0 = 0$ which is characteristic for well deformed nuclei

(iii) Fig. 10c: The γ-soft PES which has a relative maximum at $\beta = 0$ and shows a shallow valley at $\beta_0 \neq 0$ with the deeper minimum either at $\gamma = 0°$ (prolate type) or at $\gamma = 60°$ (oblate type).

(iv) Fig. 10d· The triaxial-rotor PES which is similar to the γ-soft PES but possesses a clear minimum in the triaxial region

The existing microscopic calculations of PES in the $A = 190$ and $A = 135$ mass regions yield PES of the γ-soft type without any pronounced triaxial minima [33-35]†. This result seems to be inconsistent with the present result as well as with empirical data of even-A nuclei. The evidence from even nuclei is discussed first

(a) A specific test for complete γ-softness is the degeneracy of both the 2_2^+ with the 4_1^+ state and the 3_1^+ with the 4_2^+ state of the quasi-γ-band This simultaneous degeneracy occurs for a completely γ-independent PES *no matter* what the β-dependence is [model of Wilets and Jean [37]]. In table 6, data for ^{190}Os and ^{124}Xe which have $E_{2_2^+} \approx E_{4_1^+}$ are compared with the γ-soft case and the triaxial rotor It is seen that the

TABLE 6

Comparison of theoretical and experimental energy ratios of the the quasi-γ-band

	Theory		Experiment	
	γ-soft	triaxial rotor ($\gamma = 22.2°$)	^{190}Os [a])	^{124}X [b])
$E_{2_2^+}/E_{4_1^+}$	1	1	1.02	0.96
$\frac{E_{4_2^+} - E_{2_2^+}}{E_{3_1^+} - E_{2_2^+}}$	1	2.73	2.01	1.47

[a]) Ref [13]).
[b]) Ref. [42])

measured γ-band ratios are inconsistent with complete γ-softness which, on the other hand, has been obtained approximately from microscopic calculations for ^{190}Os [ref [33])] and ^{126}Ba [ref [34])]. Also the rigid-triaxial-rotor limit is not reached, suggesting that the actual wave functions are neither sharply localized nor equally distributed in the γ-valley, but have a certain limited spread – for ^{190}Os less than for ^{124}Xe. Such wave functions would be obtained from the triaxial type of PES shown in fig. 10d

(b) A similar result has been obtained by Gneuss and Greiner [38]) and more recently by Habs *et al* [39]) based on a fit of the anharmonic-vibrator model to low-energy data. These empirical PES of nuclei in the $A = 135$ region show pronounced minima of triaxial type.

The result of the present work on odd-A nuclei points into the same direction. The question is to which extent the odd particle is able to shift the average parameters of the core The odd-A energies vary strongly as functions of γ, and, for a very γ-soft potential, one would expect large variations of γ within a family of odd-A states and also in comparison with the even neighbors A feeling for this effect can be

† A recent theoretical study on potential-energy surfaces, however, shows some triaxial minima [36]), most pronounced for nuclei with $N = 76$ and $56 \leq Z \leq 66$

obtained from results of Kumar and Baranger on even nuclei in the $A = 190$ mass region Based on calculated PES and a dynamic treatment of β and γ, they derive rms values of β and γ for the lowest excited states. Some results for ^{186}Os and ^{196}Pt are given in table 7. In the ground state band, γ_{rms} moves slightly towards $\gamma = 0°$ for ^{186}Os and towards $\gamma = 60°$ for ^{196}Pt with increasing energies; for the second 2^+ state, however, it is sharply pushed towards $\gamma = 30°$. This is just what one expects from the slopes of the triaxial-rotor energies as functions of γ (compare fig. 2, of I) in the case of γ-soft shapes. Since the energy of the 2_2^+ state comes down steeply for $\gamma \to 30°$, it tends to push the core in this direction

TABLE 7

Comparison between calculated β_{rms} and γ_{rms} values and standard β and γ fit-values of this work

	^{186}Os [a])		^{186}Os [b])		^{196}Pt [a])		^{196}Hg [b])	
	β_{rms}	γ_{rms}(deg)	β	γ(deg)	β_{rms}	γ_{rms}(deg)	β	γ(deg)
0_1^+	0.223	23.2	0 23	16	0 154	36 2	0 13	37
2_1^+	0 230	21.1			0 168	38 9		
4_1^+	0 239	19.6			0 181	40 5		
2_2^+	0 226	33 4			0 173	31 2		

[a]) Ref. [33]).
[b]) This work

In contrast to these theoretical results, the present comparison with experimental odd-A spectra indicates that the γ-deformations are rather stable. E.g. for the odd-A Au isotopes, our result is definitely in disagreement with large variations of γ comparable to those of γ_{rms} shown in table 6 One could think of a stabilisation due to the odd particle; but this would not explain why the $h_{\frac{11}{2}}$ spectrum in Au and the $h_{\frac{9}{2}}$ spectrum in Tl consistently lead to the same $\gamma = 37°$, within $\pm 2°$ or so, as the Hg cores Our conclusion is therefore that the Hg cores themselves are less γ-soft than calculated PES in this mass region and that they have probably triaxial potential minima of the kind shown in fig. 10d. A similar conclusion seems to be indicated by the present work for Os, Pt, and even-A cores around $A = 135$, although the present evidence for these cases is not as strong as for the Hg isotopes

One would like to make the conclusion more quantitative This would require, however, a calculation, similar to that of Gneuss and Greiner, for odd-A nuclei in which the odd particle is coupled to a parameterized anharmonic vibrator or at least a γ-soft vibrator (only β fixed!) and in which the parameters are fitted to experiment. This procedure would make more sense for the odd-A case than for the even-A case since there are much more data known in the low-energy region for odd-A nuclei which would check the model Unfortunately, no results of such calculations are at our disposal at the moment.

In the past, odd-A transitional nuclei have been described on a spherical basis coupling a quasiparticle to one or two phonons Such calculations have been performed on a large scale by Kisslinger and Sorensen who used RPA phonons based on the pairing-plus-quadrupole model [40]). Most published results are given for low-lying non-unique parity states, and no comparison with the present results on unique-parity states is possible

Interesting calculations have been performed recently by Paar within the Alaga model [41]) for nuclei which are three particles or three holes away from closed shells In these calculations, three-particle (hole) clusters are coupled to one and two phonons of closed-shell nuclei Anharmonicities are considered to arise exclusively from the particle-phonon coupling It will be interesting to compare the results of the triaxial-rotor model with those of the Alaga model, e g , for Au isotopes, when they become available

5. Conclusion

Stimulated by new results from heavy-ion and β-decay experiments, families of unique-parity states in transitional odd-A nuclei have been investigated in a systematic way. Although quite different types of level orders are observed in these spectra, they all appear to arise from the same physical structure This structure can be described in a relatively simple and intuitive model consisting of an odd nucleon coupled to a triaxial rotating core.

In the best experimental cases, e.g , in ^{187}Ir and ^{195}Au, 13 or more states of one family are known at low energy ($< 2\Delta$). The model calculation, reproduces *all* states in almost the right order, including high-spin *and* low-spin states. The unique-parity systems have been studied here for nuclei in the $A = 190$ and $A = 135$ mass regions Similar spectra, however, have also been seen in some lighter nuclei, and they possibly represent a general structure characteristic for weakly deformed open-shell nuclei.

The model depends only on the three parameters, β, γ, and λ_F, which have a direct physical significance and can be determined almost independently from the odd-A spectra As a function of the deformation parameter $\beta A^{\frac{1}{3}}$, the model describes different strengths of core-particle coupling intermediate between weak coupling and strong coupling, whereas the variations with γ provide the main clue for understanding the variety of different level orders observed in experiment. A most beautiful example for these changes is given by the unique-parity spectra in Ir, Au, and Tl isotopes. The gradual shape transition in this mass region from strongly deformed prolate to weakly deformed oblate shapes through a series of triaxial shapes is reflected in detail by these spectra in agreement with the present theoretical description

The puzzling result of this work is that the odd-A spectra define γ rather sharply, within $\pm 2°$ or so for cases like ^{195}Au or ^{137}Nd, and that, within this margin, these values coincide consistently with those derived from the even neighbors – the $(A-1)$ neighbor for particle and the $(A+1)$ neighbor for hole spectra. This result seems to be inconsistent with calculated potential-energy surfaces which yield very γ-soft shapes

for these transitional nuclei. Though no quantitative conclusion can be drawn at the moment, the present work strongly suggests that these nuclei are more stable than generally assumed and some of them might have collective potentials with rather pronounced minima in the triaxial region. If confirmed, this result could have serious implications concerning the calculation of potential-energy surfaces

The present work has strong applications in the field of experiment. It provides a general frame for analyzing low-energy spectra of transitional odd-A nuclei. It predicts numerous states, their energies, moments, and transition probabilities, which have not yet been measured. More experimental results are necessary to judge the range of validity of the present model. Certain discrepancies are expected due to shape fluctuations and other effects. But the present work clearly points out that there is a simple general structure behind the intricate and, so far, poorly understood odd-A spectra in the transitional regions and that the concept of triaxial nuclear deformations represents a natural way to understand their systematic behavior.

The authors thansk Dr. J. Jastrzebski for the communication of data on ^{187}Ir of the Grenoble-Swierk collaboration before publication and the permission to use them in this publication. He thanks Drs. R. M. Diamond and F. S. Stephens for their great help concerning this work and acknowledges helpful discussions with Prof. J. Rasmussen and Drs. N. Glendenning, W. J. Swiatecki, C. Gerschel, J. Gizon, D Habs, R. A. Meyer, and C. Sebille-Schück. He also thanks Drs. E Browne and R. Doebler from the Table of Isotopes group for critical comments on experimental data and thanks Dr. N. Glendenning for the hospitality of the Nuclear Theory group in Berkeley.

References

1) J. Meyer-ter-Vehn, Nucl. Phys **A249** (1975) 111
2) S. André, J Boutet, J. Rivier, J Treherne, J Jastrzebski, J Lukasiak, Z. Sujkowski and C Sebille-Schuck, Proc Int. Conf. on reactions between complex nuclei, Nashville, 1974, vol 1 eds. R L. Robonson *et al* (North-Holland, Amsterdam, 1974) p 192, Nucl Phys **A243** (1975) 229
3) C Sebille-Schuck, M. Finger, R. Foucher, J P Husson, J. Jastrzebski, V Berg, S G Malmskog, G Astner, B R. Erdal, P. Patzelt and P Siffert, Nucl. Phys **A212** (1973) 45
4) A Backlin, V Berg and S. G. Malmskog, Nucl Phys **A156** (1970) 647
5) A Backlin, G Hedin and S G Malmskog, Nucl. Phys **A169** (1971) 122
6) R H. Price, D. G. Burke and M W. Johns, Nucl. Phys **A176** (1971) 338
7) V Berg, M A Deleplanque, C Gerschel and N. Perrin, IPNO-Ph N-74-12, Inst Phys Nucl , Orsay,
V. Berg, R. Foucher and Å. Hoglund, Nucl. Phys. **A244** (1975) 462
8) H Beuscher, P. Jahn, R. M. Lieder and C. Mayer-Boricke, Z. Phys. **247** (1971) 383
9) M B Lewis and M. J Martin, Nucl Data Sheets **8** (1972) 389, 431
10) P O. Tjøm, M R Maier, D Benson, Jr , F S Stephens and R. M. Diamond, Nucl Phys **A231** (1974) 397
11) Ch Vieu, A. Peghaire and J. S Dionisio, Rev de Phys Appl. **8** (1973) 231
12) J O Newton, S D Cirilov, F. S Stephens and R. M. Diamond, Nucl Phys. **A148** (1970) 593, J O Newton, F S. Stephens and R. M. Diamond, Nucl Phys **A236** (1974) 225
13) M Sakai, Institute for Nuclear Study report INS-J-142 (1973), Univ. of Tokyo

14) D. Proetel, D. Benson, Jr, A Gizon, J. Gizon, M R. Maier, R M Diamond and F S. Stephens, Nucl. Phys. **A226** (1974) 237
15) H. Beuscher, W. F. Davidson, R. M. Lieder, A Neskaskis and C Mayer-Boricke, Phys. Rev Lett **32** (1974) 843
16) V. Berg, C Bourgeois and R Foucher, IPNO-Ph N.-75-08, Inst Phys Nucl, Orsay, and to be published in J de Phys
17) J. Meyer-ter-Vehn, F S. Stephens and R. M Diamond, Phys Rev Lett **32** (1974) 1383
18) R. K Sheline, T. Sikkeland and R N Chanda, Phys. Rev. Lett **7** (1961) 446
19) K Kumar and M. Baranger, Phys. Rev Lett **12** (1964) 73
20) C W Towsley, R Cook, D Cline and R N Horoshko, J Phys. Soc Jap Suppl. **34** (1973) 442
21) J J. Simpson, D. Eccleshall, M. J L Yates and N J. Freeman, Nucl Phys **A94** (1967) 177,
J R Kerns and J. X. Saladin, Phys Rev **C6** (1972) 1016,
M. Neiman, R. Kalish, D. R S Somayajulu, B Herskind, F Genovese and L Grodzins, Phys Lett **52B** (1974) 189
22) J R Leigh, K. Nakai, K H. Maier, F Puhlhofer, F S Stephens and R M Diamond, Nucl. Phys **A213** (1973) 1
23) E A. Henry and R A Meyer, Lawrence Livermore Laboratory report UCRL-75676 (1974)
24) R Hayano, J Chiba, M. Sekimoto, H Nakayama and K. Nakai, University of Tokyo preprint (1974)
25) J van Klinken, D Habs, H Klewe-Nebenius, K. Wisshak, G. P Nowicki, J Buschmann, S. Goring, R Lohken, H. Rebel and G Schatz, Ges f Kernforschung report KFK-1768 (1974), Karlsruhe
26) J. Gizon, A. Gizon, M. R Maier, R. M Diamond and F S. Stephens, Nucl Phys **A222** (1974) 557
27) J. Gizon, A Gizon and D J Horen, Proc Int. Conf on reactions between complex nuclei, Nashville, 1974, vol 1, ed. R L Robonson *et al.* (North-Holland, Amsterdam, 1974) p 154
28) G. P Nowicki, Ges f. Kernforschung report KFK-2017 (1974), Karlsruhe
29) P A Butler, J. Meyer-ter-Vehn, D Ward, H Bertschat, P Colombani, R M Diamond and F S Stephens, Phys Lett. **56B** (1975) 453
30) K Nakai, D. Proetel, R. M Diamond and F S Stephens, Phys Rev Lett **32** (1974) 1380
31) A Faessler, J E Galonska, U. Goetz and H C Pauli, Nucl. Phys **A230** (1974) 302
32) P. Ring and H. J. Mang, Phys. Rev Lett. **33** (1974) 1174
33) K Kumar and M Baranger, Nucl Phys. **110** (1968) 529; **A122** (1968) 273
34) D A Arseniev, A. Sobiczewski and V. G. Soloviev, Nucl Phys. **A126** (1969) 15
35) U Goetz, H C. Pauli, K Alder and K Junker, Nucl Phys **A192** (1972) 1
36) I Ragnarsson, A Sobiczewski, R K Sheline, S. E Larsson and B Nerlo-Pomorska, Nucl Phys **A233** (1974) 329
37) L. Wilets and M Jean, Phys. Rev **102** (1956) 788
38) G Gneuss and W Greiner, Nucl Phys **A171** (1971) 449
39) D Habs, H. Klewe-Nebenius, K Wisshak, R Lohken, G Nowicki and H Rebel, Z Phys **267** (1974) 149
40) L S Kisslinger and R A Sorensen, Rev Mod Phys **35** (1963) 853
41) V Paar, Nucl. Phys. **A211** (1973) 29
42) M Sakai, Institute for Nuclear Study report INS-J-146 (1974), Univ. of Tokyo,
H Kusakari, N Yoshikawa, H. Kawakami, M Ishihara, Y Shida and M Sakai, Nucl Phys **A242** (1975) 13
43) U Goetz, H. C Pauli and K. Alder, Nucl Phys **A175** (1971) 481
44) J L Wood, private communication